Journal of Chromatography, 185 (1979) 273–288

CHROM. 12,297

HIGH-PERFORMANCE SIZE-EXCLUSION LIQUID CHROMATOGRAPHY OF INORGANIC COLLOIDS

J. J. KIRKLAND

E. I. du Pont de Nemours and Company, Central Research & Development Department, Experimental Station, Wilmington, Del. 19898 (U.S.A.)

SUMMARY

High-resolution separations of inorganic colloids in the 1–50 nm range can be rapidly carried out by size-exclusion chromatography using columns of $< 10\,\mu m$ porous silica microspheres (PSM). The high efficiency of the PSM columns used in this application is the result of the rapid equilibration of slowly diffusing colloids with the porous structure of these very small particles. Subtle differences in the size characteristics of aluminosilicate sols have been measured in a few minutes with columns of $\approx 7\,\mu m$ PSM particles. The mass transfer properties of superficially porous particles (solid core, porous crust) suggest that this type of packing should also be useful for the rapid separation of slowly diffusing colloids. Size-exclusion chromatography appears to be a useful technique for characterizing a variety of both inorganic and organic colloids.

INTRODUCTION

Size-exclusion liquid chromatography (SEC, sometimes called gel permeation chromatography or gel filtration chromatography) has been widely used for separating macromolecules in solution according to their size[1–6]. However, the utility of the method for classifying colloids according to particle size has not been widely exploited. While separations of polymethylmethacrylate, polystyrene latex dispersions[7], and polysilicic acid[8,9] were reported several years ago, only recently has the SEC of particle suspensions been investigated sufficiently to allow problem solving[10–12]. Separations of colloidal particles by SEC have been carried out with long columns of relatively large porous particles[7–12]. However, work with such systems required long separation times and provide only modest resolution as result of relatively poor column efficiency. In addition, SEC separations have been largely concerned with organic colloidal particles of >20 nm formed by emulsion polymerization.

The present study was carried out to investigate the properties of small ($<10\,\mu m$) porous silica microspheres (PSM) for characterizing inorganic colloids. PSM particles with the proper pore size should have excellent mass transfer characteristics that permit the rapid separation of slowly diffusing inorganic colloids with high

resolution. Effects of particle size, pore size, and type and velocity of mobile phase on the separation of colloidal inorganic particles have been studied. The properties of superficially porous particles have also been determined for separating colloids, since the favorable mass transfer characteristics of such packings should also permit useful applications.

EXPERIMENTAL

Apparatus

The SEC apparatus and general chromatographic technique used in this study have been described[13–16]. Detection was at a wavelength of 254 nm using a DuPont Model 410 UV photometer fitted with a 1-μl detector cell[14]. Samples were introduced into columns by a Model CV-6-UHPa-C-20 microsampling valve (Valco Instruments, Houston, Texas, U.S.A.) with an external sample loop.

The PSM column packing, the column wet-fill packing methods for $<10\,\mu$m particles, and column hardware were the same as previously described[16]. Experimental chromatographic support consisting of Zipax® (DuPont) controlled surface porosity particles[17] were kindly supplied by Dr. J. J. DeStefano of DuPont's Instrument Products Division. Porasil C was obtained from Waters Assoc. (Milford, Mass., U.S.A.) and the Spherosil packings from Supelco (Bellefonte, Pa., U.S.A.). These materials were size-graded by sieving, and the fines were removed by sedimentation in methanol before use. Columns of all $> 10\,\mu$m particles were dry packed using a custom-designed machine which optimizes the widely used tap-fill column packing procedure[18].

The characteristics of column packing materials used in this study are summarized in Table I.

TABLE I
CHARACTERISTICS OF PARTICLES USED FOR SEC SEPARATIONS OF COLLOIDS

Packing designation	*Size (μm)*	*Av. pore size (nm)**	*Nitrogen surface area (m^2/g)***	*Internal porosity (ml/g)**	*Porosity (vol. %)**
PSM-500 I	7.7 ± 1.9***	22	52	0.359	44.1
PSM-500 II	7.5 ± 1.7***	20	66	0.424	48.1
PSM-800	6.0 ± 1.5***	30	34	0.426	48.3
PSM-1500	8.9 ± 1.2***	75	20	0.459	50.2
Porasil C	38–44‡‡	25	75‡	0.934	67.3
Spherosil XOB-30	32–44‡‡	60‡	50‡	—	—
Spherosil XOC-005	32–44‡‡	300‡	10‡	—	—
Experimental Zipax®	26–40‡‡	95	1.3	0.038	7.7

* Mercury intrusion.
** B.E.T.
*** Quantimet analysis, $\pm 1\sigma$, distribution weighted by volume.
‡ Reported by manufacturer.
‡‡ Semi-quantitative optical microscopy.

Samples

The silica sols used in this study were commercial or experimental samples of Ludox® colloidal silica (Du Pont), or prepared by the controlled hydrolysis of

ethyl silicate[19]. Experimental alumino-silicate sols were prepared by Dr. H. E. Bergna of DuPont's Chemicals, Dyes and Pigments Department.

Data handling

Column performance was calculated with a supplementary program on the DuPont Experimental Station PDP-10 real-time computer system[20]. Plate height values were derived from peak areas using the method suggested by James and Martin[21].

THEORETICAL BACKGROUND

Band broadening in liquid chromatography is commonly characterized by the column plate height which can be described as:

$$H = H_L + H_{SM} + H_S + H_M \tag{1}$$

where H_L, H_{SM}, H_S, and H_M are the plate height contributions resulting from longitudinal diffusion, stagnant mobile phase, stationary phase, and interparticle mobile phase mass transfer processes, respectively. These plate height factors are a general rather than a comprehensive representation of the column band-broadening processes. Extra-column peak dispersion effects are not included in eqn. 1, but are expected to behave similarly to the independent mass transfer terms, with the plate height contribution increasing linearly with flow-velocity. In SEC, the H_S stationary phase mass transfer does not contribute to plate height. In addition, the longitudinal diffusion contribution, H_L, is insignificant, since the large solute molecules normally encountered in SEC have very small diffusion coefficients. Thus, with H_L and H_S deleted from eqn. 1, the general plate height equation for SEC takes the form of:

$$H = H_{SM} + H_M \tag{2}$$

A more detailed plate height equation with expressed operational parameters takes the form of[3].

$$H = \frac{C_{SM} d_p^2 u}{D_{SM}} + \frac{1}{\left(\frac{1}{C_e d_p}\right) + \left(\frac{D_M}{C_M d_p^2 u}\right)} \tag{3}$$

where d_p = particle diameter of the packing; u = mobile phase velocity; D_M and D_{SM} are sample diffusion coefficients in the mobile and stagnant mobile phases, respectively; and C_e, C_M, and C_{SM} are coefficients of the respective dispersion terms in the plate height equation. Diffusion coefficients D_M and D_{SM} in eqn. 3 are dependent on molecular weight (or mass), therefore, band broadening is a significant function of this property.

RESULTS AND DISCUSSION

SEC with small porous particles

Effect of mobile phase velocity. The relationship in eqn. 3 suggests that the

effect of particle size is most important for very large sample particles with very small diffusion coefficients. Therefore, columns of very small (< 10 μm), totally porous particles are particularly favored when colloidal particles with extremely small diffusion coefficients are to be characterized. The particle size effect is even more important for fast SEC separations of colloids at high mobile phase velocities. Therefore, relatively short columns of small (< 10 μm) particles can be anticipated to exhibit superior resolution of colloidal inorganic dispersions for rapid characterizations.

Eqn. 3 further points out that the size of the packing particles and the diffusivity of the sample particles (a function of size) both influence the effect of mobile phase velocity (or flow-rate) on column plate height. Fig. 1 shows plate height *vs.* velocity plots for a 8-nm silica sol and acetone as determined on a column of porous silica microspheres with 22-nm pores. For the colloidal silica sample, a linear increase in plate height occurs with increasing flow-rate or mobile phase velocity. The fact that the plate height does not increase more sharply with mobile phase velocity suggests that the stagnant mobile phase diffusion coefficient D_{SM} term in eqn. 3 contributes only a small fraction to the total band-broadening. In the case of the silica sol in Fig. 1, the influence of mobile phase velocity on the plate height apparently is dominated by the relatively large plate height contribution resulting from the broad particle size distribution of the particular silica sol used. For the data in Fig. 1, the plate height equation for the colloid particles can be approximated by:

$$H = \frac{C_{SM} d_p^2 u}{D_{SM}} + C_e d_p \tag{4}$$

where in this specific case, a large C_e term apparently dominates as a result of a relatively large particle size distribution for the sol. This simplified plate height equation is often observed in SEC separations and is characteristic of many liquid

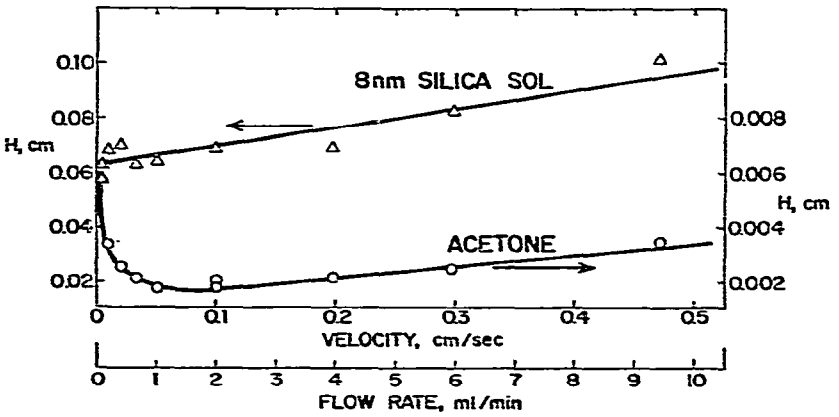

Fig. 1. Plate height *vs.* mobile phase velocity plots for porous silica microsphere column with 22-nm pores. Column: PSM-500 (7.7 μm), 15 × 0.78 cm; mobile phase: 0.1 *M* Na_2HPO_4–NaH_2PO_4, pH 8.0, detector: UV, 254 nm; sample: 6.9 μl, 10% 8 nm silica sol (Ludox®-SM) and 5 mg/ml acetone.

chromatography separations, except in those experiments which involve very low mobile phase velocities and low-molecular-weight solutes with large diffusion coefficients. In Fig. 1, the smaller acetone molecule exhibits a plate height minimum, where increased plate heights at flow-rates of less than about 1 ml/min is indicative of band broadening resulting from longitudinal diffusion (first term of eqn. 1).

The effect of mobile phase velocity on plate height can be striking when very small porous particles with larger pores are utilized in SEC, as illustrated in Fig. 2. Contrasted to Fig. 1, the steeper slope of the silica sol plate height plot suggests that band broadening is significantly affected by resistance to mass transfer in the stagnant mobile phase.

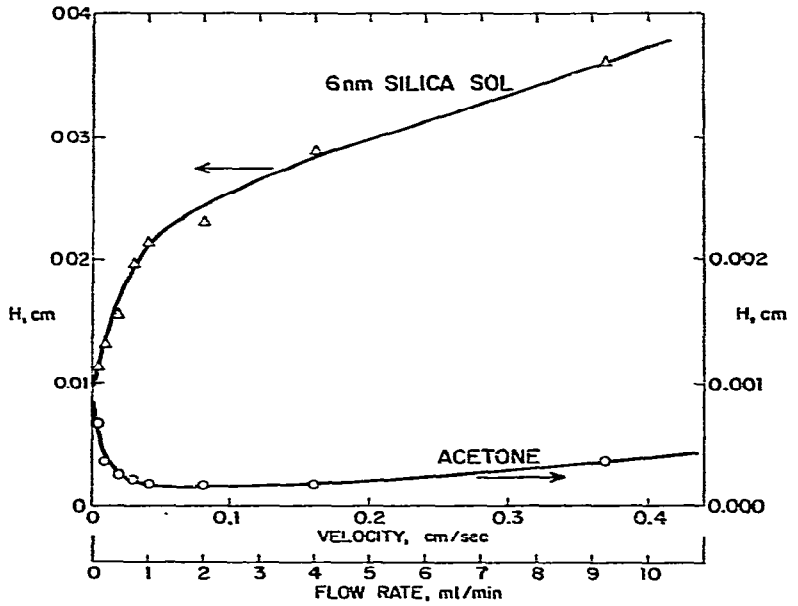

Fig. 2. Plate height *vs.* mobile phase velocity plots for porous silica microsphere column with 30-nm pores. Column: PSM-800 (6.0 μm), 10 × 0.85 cm; mobile phase, 0.001 *M* NH_4OH; detector: UV, 254 nm; sample: 6.9 μl, 2% 6 nm silica sol (Ludox®-RB) and 5 mg/ml acetone.

However, in Fig. 2 the silica sol plot shows a much smaller increase in plate height above about 1 ml/min (0.04 cm/sec) for this column of 6-μm particles with 30-nm pores. This deviation from the predicted linearity of eqn. 4 suggests the possibility of a flow-diffusive interaction within the pore structure of the column packing, as recently discussed by Van Kreveld and Van den Hoed[22]. The flow-diffusion interaction term required to explain the data in Fig. 2 should not be confused with the Giddings' coupling term[23], which only plays a role in the extra-particle mobile phase and generally involves plate height values which are considerably smaller than those of the present discussion. Also, Giddings' interparticle coupling effect usually occurs at somewhat lower mobile phase velocities than the effect exhibited here.

It should be noted that the data in Figs. 1 and 2 are presented in simple,

plate height–mobile phase velocity form rather than with the normally desired reduced parameters. This is because of the uncertainty in determining the actual silica sol diffusion coefficients within the pores of the packing; reliable values are required to calculate accurate reduced parameters. Others have shown that intraparticle and interparticle diffusion coefficients of macromolecules can be decidedly different for different size-exclusion effects; actual diffusion coefficients can change relative to the size of the sample component and pore dimension. For discussions of the restricted diffusion of molecules in various pore models, see ref. 24.

The data for the silica sol in Fig. 2 can be quantitatively fitted by an intraparticle interaction expression that includes diffusion and an empirical intraparticle flow or convection velocity[22], so that the plate height equation then takes on the approximate form:

$$H = \frac{C_{SM} d_p^2 u}{D_{SM} + uD'} + C_e d_p \tag{5}$$

where D' = the coefficient of effective mass transport within the particles resulting from intraparticle flow or convective forces. No rigorous interpretation of this intraparticle convection process is available, although it may be a function either of eddy currents or of flow through the porous structure[25]. This intraparticle convection phenomenon is apparently of little significance for larger particles with smaller pores (Fig. 1), but assumes a substantial role with very small particles of large pore size (Fig. 2). Thus, the intraparticle coupling effect is most likely observed with columns of small particles of wide pores at higher mobile phase velocities and samples with poor diffusion characteristics.

In Fig. 2, the profile of the acetone plot assumes the expected configuration and is essentially that in Fig. 1.

Particle size calibrations. Log particle size *vs.* retention volume plots for colloids in SEC systems are similar to those of soluble polymers. Fig. 3 shows the particle size calibration plot for a series of silica sols determined on a column of porous silica microspheres with 75-nm pores. Fig. 4 presents particle size calibration plots for columns of porous silica microspheres with smaller pores. In Fig. 4 the calibration plots are only approximately defined since standards of smaller silica sols were not available during this portion of the study. For spherical inorganic colloids, the linear portion of a calibration curve for packing particles with a single or a very narrow pore size is anticipated to be about 0.7 decade of particle size (ref. 6, chapter 2). This prediction is closely followed by the experimental data from this study, since the linear fractionation range of the PSM-800 column in Fig. 4 is about 3–16 nm, compared to roughly 1.5–7 nm for the PSM-500 column and an estimated 5–30 nm for the PSM-1500 column of Fig. 3.

Specific resolution (R_{sp}) and packing resolution (R_{sp}^*) values represent effective means of quantitatively characterizing the resolving power of SEC columns and column packings, respectively[26]. These values take into account both the slope of the linear particle size calibration plot, D_2, and band-broadening measured as the standard deviation of the peak, σ. The R_{sp} and R_{sp}^* values of various columns used in this study are listed in Table II. With PSM columns, R_{sp}^* values for the colloids are not unlike those previously found for polystyrene standards[26]. The much smaller

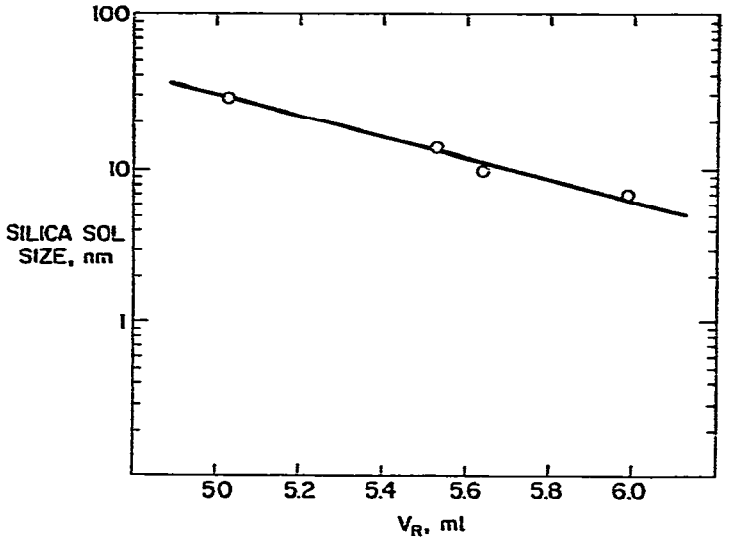

Fig. 3. Silica sol particle size calibration plot for porous silica microsphere column with 75-nm pores. Column: PSM-1500 (8.9 μm), 30 × 0.78 cm; mobile phase: 0.1 *M* Na_2HPO_4–NaH_2PO_4, pH: 8.0, flow-rate: 2.00 ml/min; pressure: 940 p.s.i.; temperature: 23°; detector: UV, 254 nm; sample: 25 μl of 2% colloid in mobile phase.

R_{sp}^* values of the controlled surface porous support (CSP) columns are due to the much smaller particle porosities compared to PSM.

Retention characteristics. Under certain conditions, silica sols of particular sizes are not eluted, depending on pore size and diameter of the porous silica

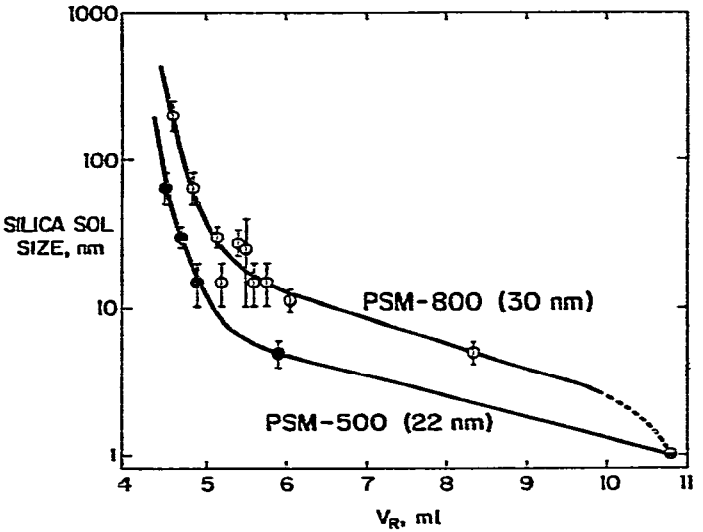

Fig. 4. Silica sol particle size calibration plots for porous silica microsphere columns. Columns: 50 × 0.62 cm, as indicated; mobile phase: 0.001 *M* NH_4OH; flow-rate: 1.00 ml/min; pressure: 1420 p.s.i.; temperature: 22°; detector: UV, 254 nm; samples: 25 μl of 2% colloid in mobile phase. ◒, acetone.

TABLE II

PERFORMANCE CHARACTERISTICS OF COLUMNS

R_{sp} = column specific resolution = $0.58/\sigma D_2$, where σ = peak standard deviation in ml at indicated flow-rate and D_2 = slope of the molecular weight calibration curve, corresponding to 3× the slope of the spherical particle size calibration curve (ref. 4), R^*_{sp} = packing resolution factor = $R_{sp}/\sqrt{L}$, where L = column length (cm).

Column packing	*Av. pore size (nm)*	*Column dimensions (cm)*	*Av. particle size (μm)*	*Flow-rate (ml/min)*	*Total plate count acetone*	*Silica sol (nm)*	R_{sp}		R^*_{sp}	
							Acetone	*Silica sol*	*Acetone*	*Silica sol*
PSM-500 II	20	15 × 0.78	7.7	2.0	6310	8	4.76*	5.92*	1.23*	0.51*
PSM-800	30	10 × 0.85	6.0	2.0	5670	6	3.29	1.90	1.05	0.60
PSM-1500	75	15 × 0.78	8.9	1.5	8030	24	1.32	0.53	0.34	0.14
Zipax®-CSP	90	100 × 0.78	30	4.0	3780	24	0.30	0.25	0.021	0.018

* Approximate values only, due to poor definition of calibration curve slope for this column (*e.g.*, Fig. 3).

particles and mobile phase type. As illustrated in Table III, PSM particles with 22-nm pores eluted all silica sols in the 5–200-nm range when 0.001 *M* ammonium hydroxide was used as the mobile phase (see Fig. 4). On the other hand, silica sols larger than about 100 nm were not eluted with 0.02 *M* phosphate buffer. These data suggest that mobile phase ions have a significant influence on the elution of silica sols from porous silica packings. In the case of dilute ammonia where the ionic strength of the solution is low, there is a relatively high negative charge on the surfaces of both the pores and the silica sol particles. In spite of this, smaller silica sol particles can enter large pores, but of course, larger sols (*e.g.*, 200 nm) are excluded because they are larger than the pores. Due to the high surface charges and strong repulsion at close ranges, particles cannot approach nor adhere to the surface and all silica sols are eluted. On the other hand, in 0.02 *M* phosphate buffer the cation concentration is sufficient to reduce the density of negative surface charges so that in the case of sol particles larger than 100 nm, Van der Waals

TABLE III

ELUTION OF SILICA FROM VARIOUS SYSTEMS

Mobile phases, A: 0.02 *M* Na_2HPO_4–NaH_2PO_4; pH 7.2; B: 0.02 *M* triethanolamine, pH 8.5 with HNO_3; C: 0.025 *M* NH_4NO_3, pH 8 with NH_4OH; D: 0.001 *M* NH_4OH; E: methanol with 0.5% of 1 *M* HNO_3; F: 0.01 *M* KNO_3 with 0.05% Aerosol OT (anionic surfactant), pH 8.0 with NH_4OH; G: 0.01 *M* KNO_3 with 0.05% Aerosol OT, pH 3.5 with HNO_3; H: 0.25% Ludox®-RM in 0.001 *M* NH_4OH; I: 0.1 *M* Na_2HPO_4–NaH_2PO_4, pH 8.0; J: 0.002 *M* triethanolamine, pH 8.6 with HNO_3.

Packing designation	*Av. particle size (μm)*	*Av. pore size (nm)*	*Mobile phase*	*Range of silica sols eluted* (nm)*	*Silica sols retained (nm)*
PSM-500	7.7	22	A	—	100–140
			D	5–200	
PSM-800	6.0	30	A	24–80	100–200
			B	5–80	
			C	—	50–200
			D	5–80	
			I	5–24	
PSM-1500	8.9	75	B	5–24	50–140
			C	24	100–140
			D	5–80	100–140
			J	24	100–500
Porasil-C	41	50	A	6–140	
			B	100–200	
			C	≤200	
Spherosil XOB-030	38	30	B	60–200	380–500
			D	50–140	
Spherosil XOC-005	38	300	A	—	100–200
			D	—	100–200
			E	—	50–140
			F	24–80	200
			G	24–50	100–140
			H	24–1400**	

* Samples, 25 μl of 0.5–2%.

** 100–140 nm sols retained about half again beyond total permeation volume.

forces are sufficient to overcome the charge repulsion and these sol particles adhere to the outside of the PSM packing particles and are not eluted.

The influence of the mobile phase on apparent silica sol size is illustrated in Fig. 5. In this case an 8-nm silica sol (Ludox®-SM) was chromatographed on a PSM-800 (30 nm) column using three different mobile phases. Based on retention, the effective size of the sol is largest in 0.001 *M* ammonium hydroxide and smallest in 0.02 *M* phosphate buffer. Reagents that most significantly affect the ionic double layer associated with colloids appear to have the largest effect on retention volume. The effect of type and concentration of mobile phase ions needs further study to better define the influence of this important parameter on colloid retention.

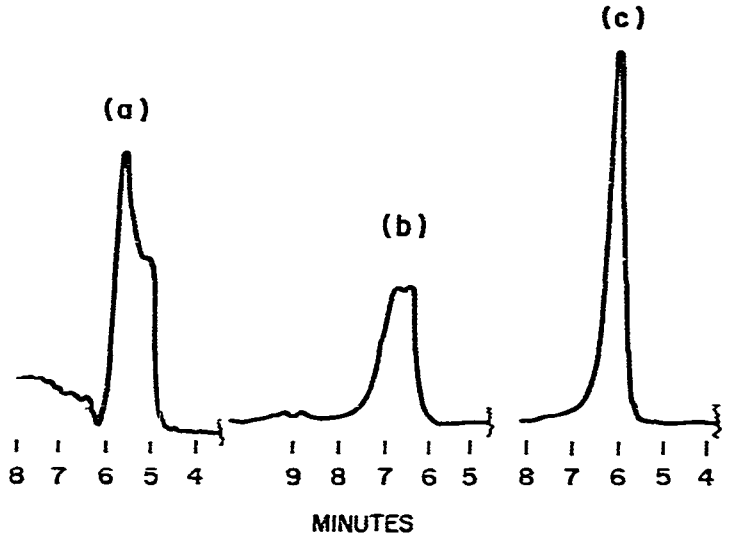

Fig. 5. Effect of mobile phase on retention. (a) 0.001 *M* NH_4OH, (b) 0.02 *M* Na_2HPO_4–NaH_2PO_4, pH 8, (c) 0.02 *M* triethanolamine, adjusted to pH 8.0 with nitric acid; column: PSM-800 (6.0 μm, 30 nm pores), 50 × 0.62 cm; flow-rate: 1.00 ml/min; detector: UV, 254 nm; sample: 25 μl of 2% 8-nm silica sol (Ludox®-SM).

Data for PSM-800 in Table III show that silica sols of larger than about 80 nm (depending on mobile phase) do not elute, while sols smaller than about 80 nm elute normally (see Fig. 4). Similarly, PSM-1500 particles with 75-nm pores elute silica sols up to sizes of about 80 nm, but sols larger than this are generally retained. These phenomena, together with results from larger silica packing particles with similar pore size (Porasil and Spherosil in Table III), suggest that silica sols of less than about 80 nm are able to move freely through the porous structure of packed beds; if pores in the packing particles are sufficiently large, solvated colloidal particles of ≈80 nm can permeate for appropriate fractionation. Solvated sol particles that are too large are excluded from the pores and elute at the normal column interstitial volume.

On the other hand, data in Table III show that when silica sols of larger than about 80 nm permeate the porous packing particles, elution generally does not occur. These results suggest that silica sols of ≈80 nm and larger are adsorbed on

the walls of the pores (regardless of type of mobile phase studied) when there is no hydrodynamic force within the pores due to fluid-flow.

This rather unusual adhesion phenomenon might be explained by the following considerations. Adhesion of a particle colliding with a pore wall occurs by the same mechanism as adhesion between two colliding particles. Apparently, only with larger silica sol particles (*i.e.*, $\gtrsim$ 80 nm) do Van der Waals attractive forces have any influence on adhesive behavior. For example, Harding[27] has found that silica particles smaller than 100 nm did not coagulate under conditions that would coagulate 320-nm particles. A steric barrier of an immobilized monolayer of water on each surface might be more effective in preventing coagulation of small silica sol particles than large ones. In the above situation observed by Harding, adhesion was between two particles. In the specific case of a silica sol particle and a pore wall, the latter is a particle of almost infinite radius. Hence, a particle as small as 70–80 nm may adhere to a pore wall under conditions where two separate particles would each have to be over 100 nm in diameter to adhere to each other on collision. Furthermore, because of steric factors, the charge density per unit area resulting from mutual charge repulsion is likely to be much larger on a bulk silica surface than within the restriction of a silica pore, making the likelihood of adhesion within the pore much greater.

Thus, silica sol particles of larger than about 80 nm have such low kinetic energy that adhesion within pores resulting from Van der Waals forces can occur, and elution does not take place. On the other hand, smaller silica sols diffuse in and out of pores normally, since they possess sufficient kinetic energy to overcome adhesion within the pores.

The data on Porasil and Spherosil in Table III indicate that their reversible retention (adhesion) of larger silica sols is specifically a function of particle pore size and is not dependent on the overall dimensions of the packing particles. Of course, if the size of the colloidal particles approaches the size of the interconnecting pores between the column bed particles, then the sol particles are permanently retained as a result of simple filtration.

Addition of a very small silica sol to the mobile phase results in the elution of silica sols which are normally unable to elute after permeating porous packing particles. For example, as shown in Table III for Spherosil XOC-005 ($\approx$ 300 nm pores; mobile phase *H*), a 120-nm silica sol eluted when the 0.001 *M* ammonium hydroxide (pH 8.5) mobile phase was "doped" with 0.25% of a 6-nm silica sol (Ludox®-RB). However, the 120-nm colloid eluted well beyond the column total permeation volume (retention volume of 80 ml, compared to 52 ml for total permeation), suggesting that some adsorption occurred during retention. Apparently, the very small silica sol modifier prevents the normal irreversible adhesion of the larger particles, perhaps by steric shielding.

The type of mobile phase can also exhibit a significant influence on the SEC of colloids. For example, as shown for wide-pore Spherosil in Table III, certain mobile phases (*e.g.*, methanol with 0.5% 1 *M* nitric acid, and 0.02 *M* triethanolamine at pH 3.0 or 8.5) do not allow the elution of silica sols even as small as 24 nm. In these cases, sols at least an order of magnitude smaller than the average pore diameter are irreversibly retained. The reason for this effect is not understood; however, such deleterious adhesion seems to be eliminated by using an

appropriate mobile phase. In the case of silica sols, 0.001 *M* ammonium hydroxide appears appropriate for many separations.

Applications. Because of the high resolution afforded by columns of small porous particles, SEC chromatograms can be obtained which show subtle differences in samples of very small inorganic colloids. Fig. 6 shows the chromatograms on three experimental aluminosilicate sols prepared by different procedures. The numbers above the peaks indicate values from the calibration in Fig. 4 corresponding to the size of silica sols eluting at the same retention volume. While no attempt was made to optimize the separating conditions, it is feasible with this system to rapidly separate 8-nm and 10-nm silica sols with unit resolution.

To insure the accuracy and reproducibility of aluminosilicate sol separations, a semi-preparative isolation was carried out in which the individual peaks of a sample similar to that in Fig. 6a were isolated and reanalyzed. To accomplish this, 200-μl aliquots of a 1% sample of the aluminosilicate sol were chromatographed with the column in a somewhat overloaded condition, and three different fractions were collected, as shown in Fig. 7. This preparative separation was carried out identically for a total of five runs, like fractions combined, and each fraction composite reseparated. Isolated composite fractions showed peaks exactly corresponding to those of the original sample, indicating that individual particle sizes remained unchanged. Apparently high-efficiency preparative SEC can be used to prepare colloids with a very narrow particle size distribution, if required.

Importantly, chromatograms such as in Fig. 6 only provide qualitative information on colloids when UV photometric devices are employed for turbidimetric detection. With such devices, detection sensitivity varies with particle size. Therefore, careful calibration is required to convert observed detector response to the desired colloid concentration for different sizes, so that a true weight fraction *versus* particle size relationship can be obtained for an unknown. Fresnel-type refractometers

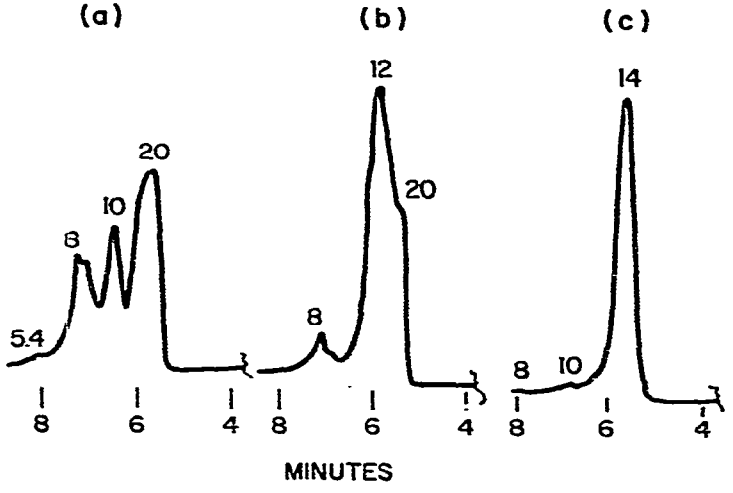

Fig. 6. Fractionation of experimental aluminosilicate sols. Conditions same as for Fig. 5, except mobile phase, 0.001 *M* NH_4OH. Three different samples, (a), (b), (c) shown.

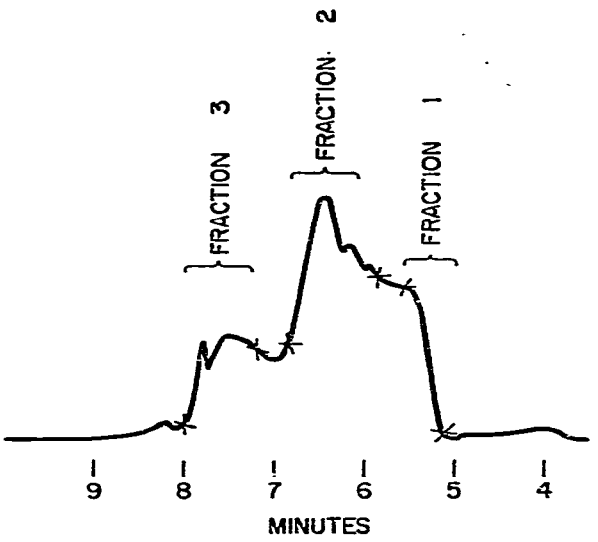

Fig. 7. Isolation of aluminosilicate sol fractions. Conditions, same as for Fig. 6, except sample: 200 μl of 1% colloid.

provide a response to various colloids that is less dependent on particle size than UV photometric detectors and therefore may be more useful for some systems. However, the response of Fresnel refractometers also varies with particle size, and empirical calibrations are still required for quantitative particle size relationships.

SEC with superficially porous particles

It can be inferred from eqns. 3 and 5 that the plate heights of SEC separations can also be decreased (and resolution increased) by using columns with smaller *effective* particles sizes. Effective reduction in particle size can be accomplished by using superficially porous particles with a relatively thin porous crust on a larger non-porous core. Such a particle with a narrow distribution of appropriate pores should provide excellent mass transfer characteristics for the SEC of slowly diffusing samples such as inorganic colloids.

Effect of mobile phase velocity. Optimum superficially porous particles for SEC separations are not presently available, but Zipax® controlled surface porosity (CSP) support CSP particle for gas and liquid chromatography[23–34] can be used as a model to confirm the utility of this type of particle for SEC. Particles of Zipax® have an average particle size of about 25 μm, and are composed of glass beads coated by multilayering[17] 200-nm silica sol particles to form a $\approx$ 1 μm porous layer. Fig. 8 shows the plate height *versus* velocity plots obtained on two 100 $\times$ 0.78 cm (200 cm total length) columns of an experimental Zipax® CPS particle for a 24-nm silica sol (Ludox®-TM) and acetone. Note the flattening off of the plate height curves for both the silica sol and acetone with increasing mobile phase velocity, in the manner of the silica sol plot in Fig. 2. However, in this case, this effect is believed to primarily result from interparticle coupling within the bed of CSP particles to improve mass transfer. The very favorable mass transfer characteristics of CSP particles is indicated by the fact that at higher mobile phase velocities, the plots in Fig. 8 show less than a three-

fold difference between the plate heights of materials that have more than a 10^3-fold difference in diffusion coefficients. The data in Fig. 8 predict that with the favorable mass transfer characteristics of superficially porous particles such as Zipax®, the SEC of very slowly diffusing species such as colloids can be carried out at relatively high mobile phase velocity without severe loss in resolution.

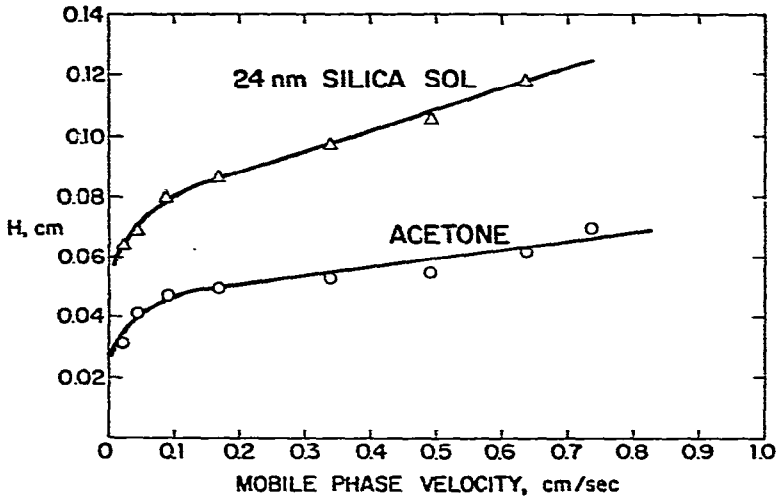

Fig. 8. Plate height *vs.* mobile phase velocity plots for superficially porous particles. Columns: two, 100 × 0.78 cm (200 cm total) experimental Zipax®, <38 μm, 95-nm pores; mobile phase: 0.02 *M* triethanolamine adjusted to pH 8 with nitric acid; detector: UV, 254 nm; sample: 50 μl of 2% 24-nm silica sol (Ludox®-TM) and 5 mg/ml acetone.

Particle size calibrations. Columns of superficially porous particles exhibit expected size *versus* retention volume plots, as illustrated in Fig. 9. In this system 200–250-nm silica sols only partially eluted from the packing, presumably because some silica sol diffuses into a few large pores and adheres. Interestingly, silica sols that are in the 80–100-nm range and might be expected to be retained within the pores by Van der Waals forces, actually elute normally. However, in the manner suggested by eqn. 5, this unexpected elution may be attributed to some convective flow within the porous crust that imparts to the large silica sol particles sufficient energy to overcome the adhesive forces within the pores of the superficially porous particles.

In Fig. 9, a data point (triangle) is shown for an unknown polysilicic acid sample prepared by deionizing a sodium silicate solution to form a very small silica sol. Comparison to the calibration plot suggests that the sol particles are about 1.5 nm in diameter. Even though polysilicic acid particles of this size tend to grow relatively rapidly, the size of such materials can be measured with good accuracy because of the ability to carry out fast separations.

The superficially porous particles used in this study obviously are not optimum for SEC, as inferred from the packing resolution data in Table II. Superior superficially porous particles for separating colloids or very high-molecular-weight

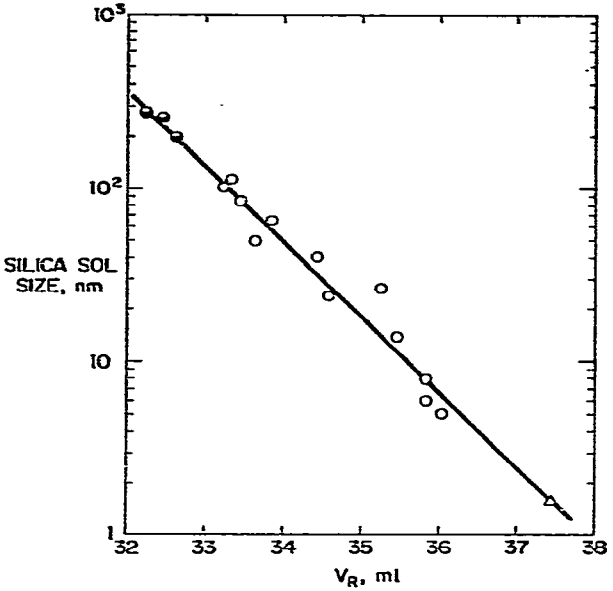

Fig. 9. Silica sol particle size calibration plot for superficially porous particles. Conditions: same as for Fig. 8, except: flow-rate; 4.00 ml/min; sample: 50 μl of 2% colloids. ○, silica sols with normal elution; ◒, silica sols with partial elution; △, polysilicic acid from deionization of sodium silicate.

macromolecules are predicted to be those with an overall diameter of about 10 μm with a porous crust of about 3 μm thickness. Nevertheless, currently available CSP packing materials can provide rapid particle size characterizations when columns of sufficient volume of packing are used. For example, a 400 × 0.78 cm column of Zipax® provides a working fractionation volume (total permeation minus total exclusion) of about 10 ml and an effective particle fractionation range of about 1–60 nm for silica sols.

CONCLUSIONS

SEC is a useful technique for characterizing a variety of colloids by size. Separation time can be minimized by using either < 10 μm PSM or ≈ 30 μm CSP superficially porous particles, depending on the particular separation goal. Columns of < 10 μm PSM particles are particularly useful for separating colloids in the 1–60-nm range, and with this approach, subtle differences in aluminosilicate sols in the 3–15-nm range have been measured in a few minutes. Columns of both the PSM and the CSP particles exhibit relatively high resolution because of the rapid equilibrium of slowly diffusing colloids with the pores of these structures. Silica sols greater than ≈ 80 nm tend to be retained within column packing pore structures into which they are able to permeate. However, larger silica sols are unable to permeate the porous structure of the packing and are eluted at the normal column total exclusion volume. The mobile phase is of special importance in the SEC of colloids, since the effective size of the colloid is a function of the nature of the liquid carrier. This parameter is of particular concern when establishing a calibration plot to characterize unknown colloids.

ACKNOWLEDGEMENTS

It is a pleasure to thank Charles H. Dilks, Jr., for his skillful assistance with the experimental work. Discussions with Drs. W. W. Yau and R. K. Iler on this work have been most helpful.

REFERENCES

1 D. D. Bly, in B. Carroll (Editor), *Gel Permeation in Polymer Chemistry, Physical Methods in Macromolecular Chemistry, 2*, Marcel Dekker, New York, 1972, Ch. 1.
2 L. R. Snyder and J. J. Kirkland, *Introduction to Modern Liquid Chromatography*, Wiley, New York, 1974, Ch. 10.
3 L. R. Snyder and J. J. Kirkland, *Introduction to Modern Liquid Chromatography*, Wiley, New York, 1974, Ch. 2.
4 L. H. Tung and J. C. Moore, in L. H. Tung (Editor), *Fractionation of Synthetic Polymers*, Marcel Dekker, New York, 1977, Ch. 6.
5 H. Determann, *Gel Chromatography*, Springer, New York, 2nd ed., 1969.
6 W. W. Yau, J. J. Kirkland and D. D. Bly, *Modern Size-Exclusion Liquid Chromatography*, Wiley, New York, 1979.
7 K. F. Krebs and W. Wunderlick, *Angew. Makromol. Chem.*, 20 (1971) 203.
8 T. Tarutani, *J. Chromatogr.*, 50 (1970) 523.
9 K. Bombaugh, in J. J. Kirkland (Editor), *Modern Practice of Liquid Chromatography*, Wiley, New York, 1971, Ch. 10.
10 H. Coll, G. R. Fague and K. A. Robillard (Eastman-Kodak, Rochester, N.Y.), *Exclusion Chromatography of Colloidal Dispersions*, unpublished results, 1975.
11 S. Singh and A. E. Hamielec, *J. Appl. Polym. Sci.*, 22 (1978) 577.
12 A. E. Hamielec and S. Singh, *J. Liquid Chromatogr.*, 1 (1978) 187.
13 J. J. Kirkland, *J. Chromatogr. Sci.*, 10 (1972) 593.
14 J. J. Kirkland, in S. C. Perry (Editor), *Gas Chromatography 1972, Montreux*, Applied Science Publ., Barking, 1973, p. 39.
15 J. J. Kirkland, *J. Chromatogr.*, 83 (1973) 149.
16 J. J. Kirkland, *J. Chromatogr.*, 125 (1976) 231.
17 J. J. Kirkland, *U.S. Patent*, 3,782,075, Jan. 1, 1974.
18 L. R. Snyder and J. J. Kirkland, *Introduction to Modern Liquid Chromatography*, Wiley, New York, 1974, p. 189.
19 W. Stöber, A. Fink and E. Bohn, *J. Colloid Interface Sci.*, 26 (1968) 62.
20 J. S. Fok and E. A. Abrahamson, *Amer. Lab.*, 7 (1975) 63.
21 A. T. James and A. J. P. Martin, *Analyst (London)*, 77 (1952) 917.
22 M. E. van Kreveld and N. van den Hoed, *J. Chromatogr.*, 149 (1978) 71.
23 J. C. Giddings, *Dynamics of Chromatography*, Marcel Dekker, New York, 1965, Ch. 2.
24 W. W. Yau, J. J. Kirkland and D. D. Bly, *Modern Size-Exclusion Liquid Chromatography*, Wiley, New York, 1979, Ch. 3.
25 C. M. Guttman and E. A. Dimarzio, *Macromolecules*, 3 (1970) 681.
26 W. W. Yau, J. J. Kirkland, D. D. Bly and H. J. Stoklosa, *J. Chromatogr.*, 125 (1976) 219.
27 R. D. Harding, *J. Colloid Interface Sci.*, 35 (1971) 172.
28 J. J. Kirkland, *J. Chromatogr. Sci.*, 7 (1969) 7.
29 J. J. Kirkland, *J. Chromatogr. Sci.*, 7 (1969) 361.
30 J. J. Kirkland, *J. Chromatogr. Sci.*, 8 (1970) 72.
31 J. J. Kirkland and J. J. DeStefano, *J. Chromatogr. Sci.*, 8 (1970) 309.
32 J. J. Kirkland, *J. Chromatogr. Sci.*, 9 (1971) 206.
33 J. J. Kirkland, *J. Chromatogr. Sci.*, 10 (1972) 129.
34 J. J. DeStefano and J. J. Kirkland, *J. Chromatogr. Sci.*, 12 (1974) 337.